Letters

Structure-Based Design of Spiro-oxindoles as Potent, Specific Small-Molecule Inhibitors of the MDM2−p53 Interaction

Ke Ding,[†] Yipin Lu,[†] Zaneta Nikolovska-Coleska,[†] Guoping Wang,[†] Su Qiu,[†] Sanjeev Shangary,[†] Wei Gao,[†] Dongguang Qin,[†] Jeanne Stuckey,[§] Krzysztof Krajewski,[‡] Peter P. Roller,[‡] and Shaomeng Wang*[,†]

Comprehensive Cancer Center and Departments of Internal Medicine, Pharmacology, and Medicinal Chemistry, and Life Sciences Institute, University of Michigan, 1500 E. Medical Center Drive, Ann Arbor, Michigan 48109, and Laboratory of Medicinal Chemistry, National Cancer Institute-Frederick, National Institutes of Health, Frederick, Maryland 21702

Received November 7, 2005

Abstract: Potent, specific, non-peptide small-molecule inhibitors of the MDM2−p53 interaction were successfully designed. The most potent inhibitor (MI-63) has a K_i value of 3 nM binding to MDM2 and greater than 10 000-fold selectivity over Bcl-2/Bcl-xL proteins. MI-63 is highly effective in activation of p53 function and in inhibition of cell growth in cancer cells with wild-type p53 status. MI-63 has excellent specificity over cancer cells with deleted p53 and shows a minimal toxicity to normal cells.

The tumor suppressor p53 plays a central role in the regulation of cell cycle, apoptosis, and DNA repair and is an attractive molecular target for cancer therapy.[1−3] Since p53 effectively suppresses oncogenesis, it is not surprising that in approximately 50% of all human cancers its function has been nullified by deletions or mutations in the DNA-binding domain of p53.[4] In the remaining 50% of human cancers, p53 retains its wild-type form, but its activity is effectively inhibited by the MDM2 oncoprotein interacting directly with p53.[5] Reactivation of the p53 function by disruption of the MDM2−p53 interaction using a non-peptide small-molecule inhibitor is now recognized as a new and promising strategy for anticancer drug design.[6−11]

The MDM2−p53 interaction involves a short helix formed by residues 13−29 of p53 and a hydrophobic cleft in MDM2.[12] Peptide-based inhibitors designed on the basis of the sequence of the p53 domain interacting with MDM2 have achieved very high binding affinities to MDM2.[13] Despite intense research efforts over the past decade in academia and the pharmaceutical industry, very few potent, non-peptide small-molecule MDM2 inhibitors have been reported until very recently.[6−11] This highlights the challenge associated with the design of non-peptide small-molecule inhibitors to target the MDM2−p53 interaction.

We have recently reported our structure-based de novo design of spiro-oxindoles as a class of potent, non-peptide small-molecule inhibitors of the MDM2−p53 interaction.[9] We showed that the most potent inhibitor **1** (Figure 1) has a K_i value of 86 nM binding to the recombinant human MDM2 protein in our fluorescence-polarization-based (FP-based) binding assay.[9] Compound **1** is effective in inhibition of cell growth in cancer cells with wild-type p53 and has selectivity over cancer cells with deleted p53 and a minimal toxicity to normal cells.[9] Compound **1** thus represents a promising lead compound for further optimization. Herein, we wish to report our further structure-based optimization for this class of compounds as inhibitors of the MDM2−p53 interaction.

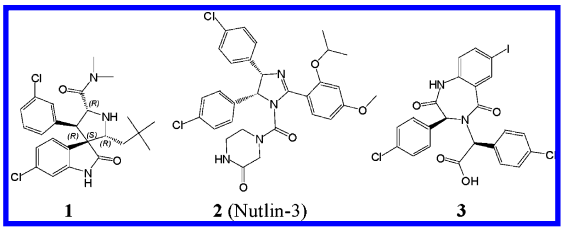

Figure 1. Recently reported potent non-peptide inhibitors of the MDM2−p53 interaction.

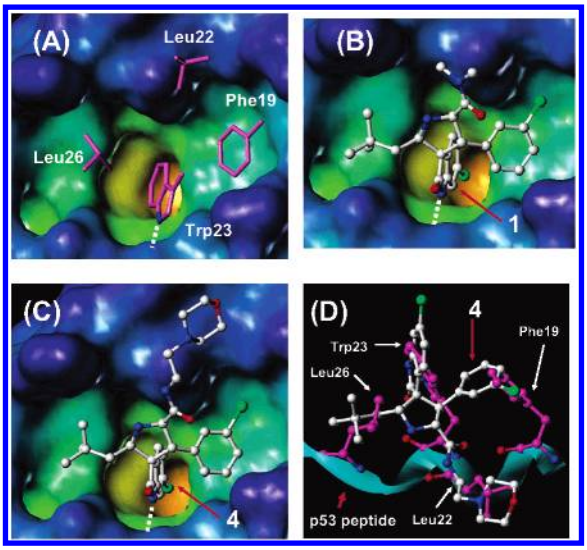

Figure 2. Structure-based design of potent small-molecule inhibitors to mimic Phe19, Trp23, Leu26, and Leu22 residues in p53. (A) X-ray structure of the p53−MDM2 complex shows that in addition to Phe19, Trp23, and Leu26, Leu22 in p53 was also shown to play a role for the interaction between p53 and MDM2. MDM2 binding site is color-coded according to the cavity depth (buried regions are coded in yellow, and solvent-exposed regions are coded in blue), and the side chains of four key residues in p53 are depicted purple in stick model. (B, C) Predicted binding models of **1** and **4** complexed with MDM2 using the GOLD program. For both compounds, carbons are in white, nitrogens in blue, chloride in green, and oxygens in red. Hydrogen bonds are depicted with a dashed yellow line. (D) Superposition of compound **4** to the p53 peptide conformation in the crystal structure of p53 peptide in complex with MDM2. Four residues, Phe19, Leu22, Trp23, and Leu26, in p53 are colored in purple. For compound **2**, the same colors are used to color-code atoms as in panel C.

X-ray crystallography revealed that the interaction between p53 and MDM2 involves primarily three hydrophobic residues (Phe19, Trp23, and Leu26) from a short α-helix in p53 and a small but deep hydrophobic pocket in MDM2 (Figure 2A).[12] Those recently reported potent non-peptide inhibitors of the

* Corresponding author. Phone: 734-615-0362. Fax: 734-647-9647. E-mail: shaomeng@umich.edu.
[†] Comprehensive Cancer Center and Departments of Internal Medicine, Pharmacology, and Medicinal Chemistry, University of Michigan.
[§] Life Sciences Institute, University of Michigan.
[‡] National Cancer Institute-Frederick.

10.1021/jm051122a CCC: $33.50
Published on Web 05/13/2006

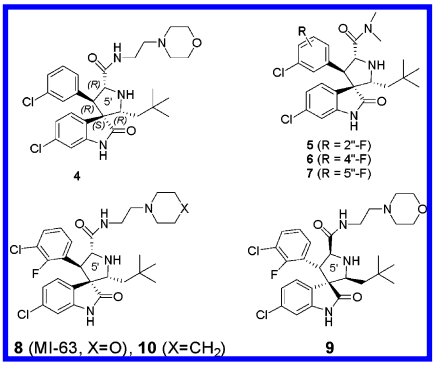

Figure 3. Designed new inhibitors of the MDM2−p53 interaction.

MDM2−p53 interaction, including the spiro-oxindole (**1**),[9] Nutlin-3 (**2**),[8] and the benzodiazepinedione **3**[10] (Figure 1), are all designed to mimic the Phe19, Trp23, and Leu26 residues in p53 and their interactions with MDM2.

Although those non-peptide inhibitors achieve high binding affinities to MDM2, they are still significantly less potent than the most potent peptide-based inhibitors. Compound **1**, for example, is 100 times less potent than the most potent peptide-based inhibitor in our binding assay.[9] This suggests that there may be additional interaction between MDM2 and those peptide-based inhibitors[13] that is not captured by these non-peptide inhibitors. Analysis of the X-ray structure[12] of the MDM2−p53 complex showed that in addition to the Phe19, Trp23, and Leu26 residues in p53, a fourth residue, Leu22, also appears to play an important role in the overall interaction between p53 and MDM2 (Figure 2A), a suggestion that finds support in results from mutation analysis[14] and alanine scanning of p53 peptides.[15] Since compound **1** was designed to mimic Phe19, Trp23, and Leu26 residues in p53, we reasoned that further optimization of compound **1** to capture the additional interaction between Leu22 in p53 and MDM2 should yield new inhibitors with higher affinity.

To test this idea, we superimposed the modeled structure[9] of compound **1** bound to MDM2 on the crystal structure[12] of the MDM2−p53 complex and showed that the 5′-carbonyl carbon of compound **1** is within 2 Å of the backbone carbonyl carbon of Leu22 in p53. This suggests that an appropriate group could be attached to this site in compound **1** to mimic Leu22 in p53. Unlike Phe19, Trp23, and Leu26, Leu22 is not buried deeply inside the binding pocket in MDM2 and is in fact partially exposed to solvent in the crystal structure.[12] This provides an opportunity to deploy a chemical group containing some polar moieties at this position not only to mimic the hydrophobic interaction of Leu22 in p53 with MDM2 but also to improve physiochemical properties of the resulting compounds such as aqueous solubility.

On the basis of these considerations, we have designed compound **4** (Figure 3), in which the *N*,*N*-dimethylamine in **1** is replaced by a 2-morpholin-4-yl-ethylamine group, a chemical group that has been extensively used in drug design. The binding model predicted by the GOLD program[16] for compound **4** (Figure 2C,D) shows that the carbon atoms in the morpholine ring, together with the two carbon linker between the morpholine ring and the 5′-carbonyl group in compound **4** closely mimic Leu22 in p53 in its interaction with MDM2. In addition, the oxygen atom in the morpholine ring is in close proximity to the positively charged amine group in Lys90 in MDM2, suggesting the possibility of hydrogen bonding. Indeed, the positively charged amino group in Lys90 in MDM2 was shown to have a strong charge−charge interaction with the negatively

Scheme 1. Synthesis of compounds **4**, **8**, and **10**[a]

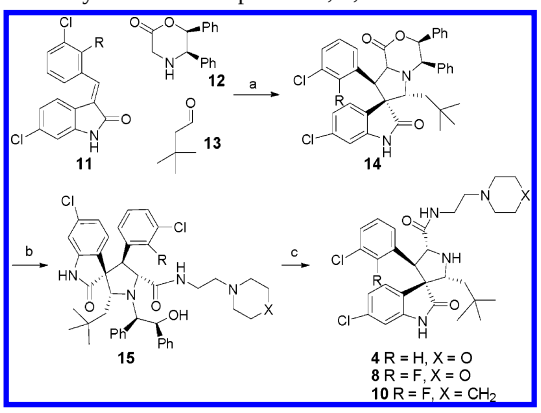

[a] Reagents and conditions: (a) 4 Å molecule sieves, toluene; (b) 2-morpholin-4-yl-ethylamine/THF(or 1-(2-aminoethyl)-piperidine/THF), RT; (c) $Pb(OAc)_4$, CH_2Cl_2−MeOH (1:1), 0 °C.

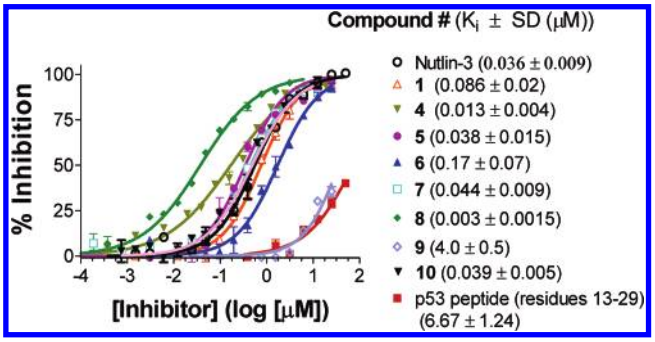

Figure 4. Competitive binding curves of small-molecule inhibitors to recombinant human MDM2 protein as determined using a fluorescence-polarization-based binding assay.

charged carboxylic group of the Glu17 in p53 in the crystal structure.[12] Hence, compound **4** not only mimics the four hydrophobic residues (Phe19, Leu22, Trp23, Leu26) in p53 (Figure 2D) for their interaction with MDM2 but also may capture the interaction between Glu17 in p53 and Lys90 in MDM2. Indeed, the GOLD program predicted that compound **4** binds more tightly to MDM2 than compound **1** based upon the predicted binding models for these two compounds.

Compound **4** was synthesized stereospecifically via a route (Scheme 1) in which the key step is an asymmetric 1,3-dipolar cycloaddition reaction.[9,17] Compound **4** was determined to bind to MDM2 with a K_i of 13 nM in our FP-based binding assay (Figure 4). Consistent with the modeling prediction, compound **4** is 6 times more potent than **1**, providing support for our design strategy.

Modeling suggests that the 4′-(*m*-chlorophenyl) ring in compounds **1** and **4** occupies a hydrophobic pocket in MDM2 (Figure 2B,C) and mimics Phe19 in p53 (Figure 2A,D). Fluorine substitution on a phenyl ring has been used frequently as an effective strategy to increase the metabolic stability of drug molecules, and we have sought to investigate the effect on binding to MDM2 of a fluoro substituent on the 4′-(*m*-chlorophenyl) in **1**. Compounds **5**, **6**, and **7** (Figure 3), in which the fluoro substituent is, respectively, at the 2, 4, or 5 position of the 4′-(*m*-chlorophenyl) ring, were synthesized using our published method[9,17] and tested for their binding affinities to MDM2. As can be seen from Figure 4, a fluorine substitution at C4 (compound **6**) results in a 2-fold reduction in binding affinity to MDM2, but substitution at C2 (compound **5**) or C5 (compound **7**) improves the binding affinity of the resulting compounds by a factor of 2. With compound **4** as the template,

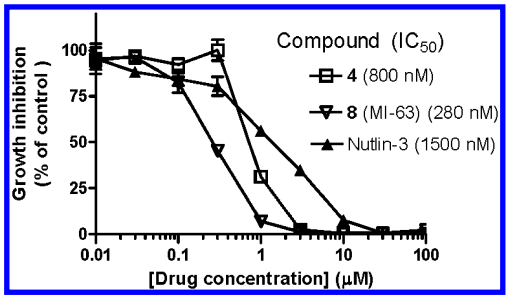

Figure 5. Inhibition of cell growth as determined by WST assay in prostate cancer LNCaP cells with wild-type p53.

compound **8**, with the 2-morpholin-4-yl-ethylamine group, was designed and synthesized. Compound **8** was determined to bind to MDM2 with a K_i value of 3 nM (Figure 4).

Compound **8** contains four chiral centers and modeling predicts that the binding of **8** to MDM2 is stereospecific. To test this prediction, we have synthesized compound **9** (Figure 3), an enantiomer of **8**, and determined that **9** has a K_i of 4.0 μM binding to MDM2 (Figure 4). Hence, **9** is 1000-times less potent than **8**, confirming stereospecific binding of **8** to MDM2.

To investigate the importance of the oxygen atom in the morpholine ring in compound **8** for binding to MDM2, we have designed and synthesized compound **10**, in which the oxygen atom was replaced by a carbon atom. Compound **10** has a K_i value of 39 nM, 13-times less potent than compound **8**, confirming the significant contribution of this oxygen atom for binding to MDM2.

Nutlin-3 was probably the most potent, cell-permeable non-peptide inhibitor of the MDM2−p53 interaction reported to date.[8] It was determined that Nutlin-3 has a K_i value of 36 nM binding to MDM2 in our binding assay (Figure 4). Hence, compound **8** is 12 times more potent than Nutlin-3 and 2000-times more potent than the natural p53 peptide (Figure 4).

These inhibitors were designed to mimic the short α-helix in p53 and to compete with p53 for interaction with MDM2. This kind of interaction, involving a surface pocket in one protein and a short α-helix in its binding partner is also observed in the interactions of the anti-apoptotic proteins Bcl-2/Bcl-xL with the pro-apoptotic Bcl-2 members such as Bid, Bad, Bak, and Bax proteins.[18] Using our established and sensitive FP-based assays for Bcl-2 and Bcl-xL proteins (Supporting Information), we have investigated whether **8** binds to these two proteins. It was found that **8** does not show a significant binding to either Bcl-2 or to Bcl-xL protein at concentrations as high as 50 μM, revealing a more than 10 000-fold specificity for MDM2 protein over Bcl-2/Bcl-xL proteins.

Potent, specific, and cell-permeable small-molecule inhibitors of the MDM2−p53 interaction are predicted to inhibit cell growth effectively in cancer cells with wild-type p53.[7−9] Furthermore such an inhibitor should have a minimal activity in cancer cells with mutated or deleted p53. Using Nutlin-3 as a positive control, we have evaluated **4** and **8** for their ability to inhibit cell growth in LNCaP prostate cancer cells with wild-type p53.[19] Compounds **4** and **8** and Nutlin-3 are indeed effective in inhibition of cell growth and achieve IC_{50} values of 800, 280, and 1500 nM, respectively, in inhibition of cell growth in LNCaP cells (Figure 5). Consistent with its higher binding affinity to MDM2, **8** is 3-times more potent than **4** and 5-times more potent than Nutlin-3 in the cell growth assay. To test the cellular specificity of **8**, we have evaluated it in human prostate cancer PC-3 cells with deleted p53[19] and found that it has an IC_{50} value of 18 μM, thus displaying an excellent

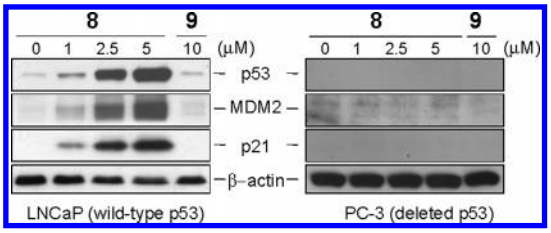

Figure 6. Western blotting analysis of p53, MDM2, and $p21^{cip1/waf1}$ proteins in LNCaP and PC-3 prostate cancer cells when treated with compounds **8** and **9** for 24 hours.

cellular specificity (Supporting Information). To evaluate its therapeutic potential further, we have tested **8** in normal prostate epithelial cells and determined that it has minimal toxicity to normal prostate epithelial cells at concentrations as high as 5 μM.

A potent small-molecule inhibitor of the MDM2−p53 interaction would be expected to activate p53, resulting in an increase in the levels of p53 in cells with wild-type p53 but not in cells with mutated or deleted p53. In addition, activation of p53 should lead to induction of p21 cyclin-dependent kinase inhibitor 1 (*$p21^{cip1/waf}$*) and *MDM2*, two p53 targeted genes, and result in an increase in the levels of $p21^{cip1/waf}$ and MDM2 proteins.[8] To test these predictions, we have examined the levels of p53, MDM2, and $p21^{cip1/waf}$ proteins by Western blotting analysis in LNCaP and PC-3 cancer cells when treated with **8** and **9**. Consistent with predictions, compound **8** causes a dose-dependent increase in the levels of p53, MDM2, and $p21^{cip1/waf}$ proteins in LNCaP cells (Figure 6), indicating a strong activation of p53. In direct comparison, **9** with a weak binding affinity to MDM2 has a minimal effect at concentrations as high as 10 μM. Since MDM2 protein is an E3 ubiquitin ligase and is known to effectively degrade p53 protein upon binding,[5] the very high levels of p53 and MDM2 protein in LNCaP cells treated with **8** suggest that MDM2 protein is unable to degrade p53 protein when blocked by **8**. Furthermore, both **8** and **9** do not increase the levels of p53, MDM2, and $p21^{cip1/waf}$ proteins in PC-3 cells with deleted p53 status (Figure 6), indicative of the lack of p53 activation.

In summary, we have successfully designed a class of high-affinity, specific, cell-permeable, non-peptide small-molecule inhibitors of the MDM2−p53 interaction using structure-based design strategy. The most potent inhibitor (**8**), which was named MI-63 (MDM2 inhibitor 63), has a K_i value of 3 nM binding to MDM2 and is more than 2000-times more potent than the natural p53 peptide (residues 13−29). MI-63 displays a high stereospecificity and is very selective in blocking the MDM2−p53 interaction rather than the Bcl-2(Bcl-xL)−Bid interaction. MI-63 is highly effective in activation of p53 function and in inhibition of cell growth in LNCaP prostate cancer cells with wild-type p53. In addition, MI-63 shows an excellent selectivity over PC-3 prostate cancer cells with deleted p53 and has minimal toxicity to normal cells. In view of all these observations, MI-63 can be regarded as a specific, promising, non-peptide small-molecule inhibitor of the MDM2−p53 interaction. This present study provides a clear example that structure-based strategy can be successfully employed in the design of potent, specific, drug-like, non-peptide small-molecule inhibitors to target protein−protein interactions.

Acknowledgment. We are grateful for the financial support from the National Cancer Institute, National Institutes of Health (Grants R01CA121279, P50CA069568, P50CA097248, and P30CA046592), and from Ascenta Therapeutics Inc.

Supporting Information Available: An experimental section including the information on the synthesis and chemical data for compounds **4**−**10**, molecular modeling methods and results for **8**, the experimental procedure for the fluorescence polarization-based binding assay, and details on the cellular assays and results. This material is available free of charge via the Internet at http://pubs.acs.org.

References

(1) Levine, A. J. p53, the cellular gatekeeper for growth and division. *Cell* **1997**, *88*, 323−331.

(2) Vogelstein, B.; Lane, D.; Levine, A. J. Surfing the p53 network. *Nature* **2000**, *408*, 6810, 307−310.

(3) Vousden, K. H.; Lu, X. Live or let die: the cell's response to p53. *Nat. Rev. Cancer* **2002**, *2*, 594−604.

(4) Hainaut, P.; Hollstein, M. p53 and human cancer: the first ten thousand mutations. *Adv. Cancer Res.* **2000**, *77*, 81−137.

(5) Wu, X.; Bayle, J. H.; Olson, D.; Levine, A. J. The p53-mdm-2 autoregulatory feedback loop. *Genes Dev.* **1993**, *7* (7A), 1126−1132.

(6) Chene, P. Inhibiting the p53-MDM2 interaction: an important target for cancer therapy. *Nat. Rev. Cancer* **2003**, *3*, 102−109.

(7) Vassilev, L. T. p53 activation by small molecules: application in oncology. *J. Med. Chem.* **2005**, *48*, 4491−4499.

(8) Vassilev, L. T.; Vu, B. T.; Graves, B.; Carvajal, D.; Podlaski, F.; Filipovic, Z.; Kong, N.; Kammlott, U.; Lukacs, C.; Klein, C.; Fotouhi, N.; Liu, E. A. In vivo activation of the p53 pathway by small-molecule antagonists of MDM2. *Science* **2004**, *303*, 844−848.

(9) Ding, K.; Lu, Y.; Nikolovska-Koleska, Z.; Qiu, S.; Ding Y.; Gao, W.; Stuckey, J.; Roller, P. P., Tomita, Y.; Deschamps, J. R.; Wang, S. Structure-based design of potent non-peptide MDM2 inhibitors. *J. Am. Chem. Soc.* **2005**, *127*, 10130−10131.

(10) Grasberger, B. L.; Lu, T.; Schubert, C.; Parks, D. J.; Carver, T. E.; Koblish, H. K.; Cummings, M. D.; LaFrance, L. V.; Milkiewicz, K. L.; Calvo, R. R.; Maguire, D.; Lattanze, J.; Franks, C. F.; Zhao, S.; Ramachandren, K.; Bylebyl, G. R.; Zhang, M.; Manthey, C. L.; Petrella, E. C.; Pantoliano, M. W.; Deckman, I. C.; Spurlino, J. C.; Maroney, A. C.; Tomczuk, B. E.; Molloy, C. J.; Bone, R. F. Discovery and cocrystal structure of benzodiazepinedione HDM2 antagonists that activate p53 in cells. *J. Med. Chem.* **2005**, *48*, 909−912.

(11) Yin, H.; Lee, G.-I.; Park, H.-S.; Payne, G. A.; Rodriguez, J. M.; Sebti, S. M.; Hamilton, A. D. Terphenyl-based helical mimetics that disrupt the p53/HDM2 Interaction. *Angew. Chem., Int. Ed.* **2005**, *44*, 2704−2707.

(12) Kussie, P. H.; Gorina, S.; Marechal, V.; Elenbaas, B.; Moreau, J.; Levine, A. J.; Pavletich, N. P. Structure of the MDM2 oncoprotein bound to the p53 tumor suppressor transactivation domain. *Science* **1996**, *274*, 948−953.

(13) Garcia-Echeverria, C.; Chene, P.; Blommers, M. J. J.; Furet, P. Discovery of potent antagonists of the interaction between human double minute 2 and tumor suppressor p53. *J. Med. Chem.* **2000**, *43*, 3205−3208.

(14) Lin, J.; Chen, B.; Elenbass, B.; Levine, A. J. Several hydrophobic amino acids in the p53 amino-terminal domain are required for transcriptional activation, binding to mdm-2 and the adenovirus 5 E1B 55-kD protein. *Genes Dev.* **1994**, *8*, 1235−1246.

(15) Picksley, S. M.; Vojtesek, B.; Sparks, A.; Lane, D. P. Immunochemical analysis of the interaction of p53 with MDM2;- -fine mapping of the MDM2 binding site on p53 using synthetic peptides. *Oncogene* **1994**, *9*, 2523−2529.

(16) Jones, G.; Willett, P.; Glen, R. C.; Leach, A. R.; Taylor, R. Development and validation of a genetic algorithm for flexible docking. *J. Mol. Biol.* **1997**, *267*, 727−748.

(17) Ding, K.; Wang, G.; Deschamps, J. R.; Parrish, D. A.; Wang, S. Synthesis of spirooxindoles via asymmetric 1,3-dipolar cycloaddition. *Tetrahedron Lett.* **2005**, *46*, 5949−5951.

(18) Oltersdorf, T.; Elmore, S. W.; Shoemaker, A. R.; Armstrong, R. C.; Augeri, D. J.; Belli, B. A.; Bruncko, M.; Deckwerth, T. L.; Dinges, J.; Hajduk, P. J.; Joseph, M. K.; Kitada, S.; Korsmeyer, S. J.; Kunzer, A. R.; Letai, A.; Li, C.; Mitten, M. J.; Nettesheim, D. G.; Ng, S.; Nimmer, P. M.; O'Connor, J. M.; Oleksijew, A.; Petros, A. M.; Reed, J. C.; Shen, W.; Tahir, S. K.; Thompson, C. B.; Tomaselli, K. J.; Wang, B.; Wendt, M. D.; Zhang, H.; Fesik, S. W.; Rosenberg, S. H. An inhibitor of Bcl-2 family proteins induces regression of solid tumours. *Nature* **2005**, *435*, 677−681.

(19) Fan, R.; Kumaravel, T. S.; Jalali, F.; Marrano, P.; Squire, J. A.; Bristow, R. G. Defective DNA strand break repair after DNA damage in prostate cancer cells: implications for genetic instability and prostate cancer progression. *Cancer Res.* **2004**, *64*, 8526−8533.

JM051122A